

Vibration Isolation and Transmissibility Characteristics of Passive Sequential Damper

M.S. Patil, M.K. Hada, S.Y. Bhawe, and S.G. Joshi

Institute of Armament Technology, Pune-411 025

ABSTRACT

This paper presents a half-car model (4-degrees-of-freedom) employing nonlinear passive sequential damper. The vibration isolation and transmissibility effect on the vehicle's centre of gravity (C.G.) has been studied. The results have been compared for transmissibility, displacement, and velocity transient response for half-car model having nonlinear passive sequential hydropneumatic damper under different terrain excitation.

Keywords: Dampers, damping, damping force, passive vibration isolator, vehicle isolator, passive sequential damper, semi-active vehicle suspension, tunable damper, variable damping, fixed damping, fluid flow, hydraulic damper, damper-control scheme

NOMENCLATURE

A_{n1}	Area of piston orifice	I_p	Pitch inertia of sprung mass
A_{n2}	Area of base orifice	K_s	Spring stiffness
A_p	Area of piston	K_t	Tyre stiffness
A_r	Area of piston rod	l_f	Distance from front-end to mass centre
C	Damping rate	l_i	Initial distance before obstacle
C_{d1}	Coefficient of discharge of fluid flow through piston orifice	l_r	Distance from rear-end to mass centre
C_{d2}	Coefficient of discharge of fluid flow through base orifice.	m_u	Unsprung mass
F_a	Damping force due to gas column in reserve chamber	m_s	Sprung mass
F_d	Damping force due to orifice flow in rebound and compression chamber	n	Number of orifices
F_D	Total damping force	P_{12}	Pressure differential across rebound and compression chamber
		P_{32}	Pressure differential across reserve and compression chamber
		P_{30}	Pressure differential in reserve chamber

Revised 26 May 2003

P_0	Hydraulic pressure corresponding to static equilibrium
$(P_{12})_0$	Preset pressure differential
R	Half-round obstacle radius
Sign	Signum function
tf	Pressure limiting tuning factor
V_0	Initial gas volumes at static equilibrium
V	Vehicle forward speed
ω	Excitation frequency
ω_n	Undamped natural frequency
X_r	Input amplitude
χ_s	Sprung mass displacement
$\dot{\chi}_s$	Sprung mass velocity
$\ddot{\chi}_s$	Sprung mass acceleration
χ_u	Unsprung mass displacement
$\dot{\chi}_u$	Unsprung mass velocity
Z	Relative displacement
\dot{Z}	Relative velocity
ν	Polytropic constant
ρ	Mass density of fluid
ξ	Damping factor
θ_p	Pitch displacement

SUBSCRIPTS

r	Rear axle
f	Front axle

1. INTRODUCTION

The inherent performance limitations of passive vibration isolators, specifically due to fixed damping have been well-established^{1,2}. A heavily damped vehicle suspension system tends to control the amplitude of vibration response only when the frequency of the base disturbance is around the natural frequency of the system. While the vibration isolation performance of the heavily damped passive suspension is deteriorated

considerably in the higher frequency range, a lightly damped suspension is desirable when the disturbance frequencies are beyond the natural frequency. However, it yields a poor response corresponding to the vehicle resonance.

To overcome these inherent limitations, dampers with certain valving mechanism have been developed to limit the damping force corresponding to higher velocities. Such dampers exhibit high damping coefficient when relative velocity and pressure differential across the piston is low. The damping coefficient is reduced due to fluid flow through the open blow-off valves when the relative velocity and pressure differential exceeds certain preset value.

Semi-active vehicle suspensions offer a compromise between the performance benefits of an active and the simplicity of the passive suspension. A semi-active vehicle suspension requires only low-level electrical power for necessary signal processing and can provide considerable improvement in vehicle ride. Karnopp¹ proposed a semi-active damper employing a force generator based on sky-hook control. Although hardware implementation of such a system is considerably simpler than an active suspension, the realisation of semi active damping requires comprehensive instrumentation package and control devices. Moreover, measurement of certain semi-active control variables may possess complexities, specifically for low excitation frequencies^{1,2}. Semi-active on-off control yields a large magnitude of jerk around the discontinuity between the on-off states. Thus, the costs, complexities and the chatter associated with the semi-active on-off control may still be prohibitive for its general application.

The passive sequential damper taken for dynamic response analysis in this paper is a tunable damper with variable damping. In this mechanism, the control scheme employs external pressure control valves to modulate the flow through orifices based upon pressure differential across the damper piston. The damper does not require sensors and signal processing as in the case of semi-active sequential damper and offers tunable damping characteristics to suit changing applications and road profile. The vibration

isolation performance of the vehicle suspension employing the tunable damper is investigated through computer simulation of a 4-DOFs half-car vehicle system.

2. MATHEMATICAL MODELLING OF CONSTANT-ORIFICE & PASSIVE SEQUENTIAL DAMPERS

Hydraulic orifice dampers, within the vehicle suspension, are often modelled as quadratic dampers, assuming constant orifice area. Figure 1 shows the schematic of a passive hydraulic damper (constant

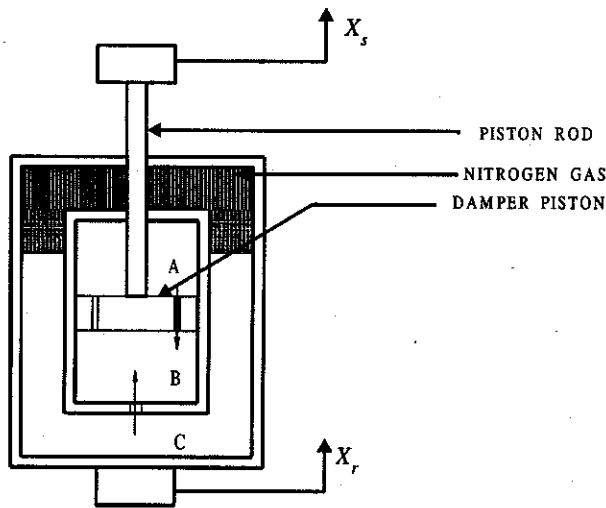


Figure 1. Constant-orifice damper showing A as rebound chamber, B as compression chamber, and C as reserve chamber.

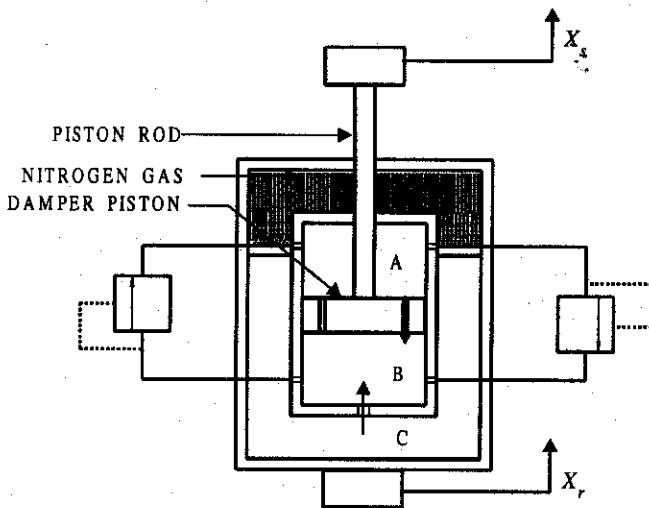


Figure 2. Sequential damper showing A as rebound chamber, B as compression chamber, and C as reserve chamber.

orifice) and the Fig. 2 shows the schematic of a passive sequential damper.

In the formulation of the analytical modelling of dampers, the following assumption are made:

- (a) Fluid flow is considered as turbulent
- (b) Seal friction and leakages are neglected
- (c) Effect due to temperature changes is negligible
- (d) Gas obeys polytropic process in reserve chamber
- (e) High bulk modulus for hydraulic fluid

The total dynamic damping force F_D generated by the hydraulic damper due to pressure differential across the damper piston⁶ is expressed as:

$$F_D = P_{12} A_p + P_{32} A_r - P_{30} A_r \quad (1)$$

Since in most orifices, the fluid flow occurs at high Reynolds numbers, the flow through orifice is considered as turbulent. At high Reynolds numbers, the pressure drop across the orifice is caused by the acceleration of fluid particles from the upstream velocity to the higher jet velocity. The flow across the orifice is streamlined and Bernoulli's equation can be applied in this region to find out the pressure differential P_{12} and P_{32} across the piston and cylinder base orifice³. In turbulent flow, the damping force results due to fluid flow through the orifices. The pressure differential equations for turbulent flow conditions are given as

$$P_{12} = \frac{\rho}{2n^2 C^2 d_1} \left[\frac{A_p}{A_{n1}} \right]^2 |\dot{Z}| \dot{Z} \quad (2)$$

and

$$P_{32} = \frac{\rho}{2C^2 d_2} \left[\frac{A_r}{A_{n2}} \right]^2 |\dot{Z}| \dot{Z} \quad (3)$$

The relationship between the pressure differential in reserve chamber and relative compression/expansion of the gas column P_{30} can be expressed as

$$P_{30} = \left\{ \frac{(V_0 + A_r Z)^y - V_0^y}{(V_0 + A_r Z)^y} \right\} P_0 \quad (4)$$

Substituting the Eqns (2), (3), and (4) in the Eqn (1), the total dynamic damping force due to hydraulic damper is obtained as

$$F_d = (A - B) \quad (5)$$

where

$$A = \frac{\rho}{2} \left[\frac{A_p}{n^2 C_{d1}^2} \left(\frac{A_p}{A_{n1}} \right)^2 + \frac{A_r}{C_{d2}^2} \left(\frac{A_r}{A_{n2}} \right)^2 \right] |\dot{Z}| \dot{Z}$$

$$B = \left\{ \frac{(V_o + A_r Z)^v - V_o^v}{(V_o + A_r Z)^v} \right\} P_o A_r$$

From the Eqn (5) it can be seen that the total dynamic force developed by the hydraulic damper comprises damping force associated with orifice flow, F_d , and a nonlinear restoring force, F_a , due to gas column. The damping force, F_d , is proportional to low/medium relative velocity and is proportional to square of relative velocity at higher relative velocities across the damper, and the restoring force, F_a , is dependent upon the relative displacement. The Eqn (5) shows that magnitude of damping force becomes predominant around high velocities, and thus yields poor vibration isolation performance. The damping force expressed by the Eqn (5) tends to decrease the amplitude of mass acceleration only during a part of vibration cycle while amplitude of mass acceleration increases in the remaining part of vibration cycle due to passive damping^{1,2}. Thus due to inherent limitations of a vibration isolator comprising passive hydraulic damper, a sequential hydraulic damper with tunable damping characteristics has been developed.

It has been shown that damping force tends to attenuate the mass acceleration only when damping force opposes relative displacement of the isolator¹. An on-off sky-hook damper control scheme, based upon the sign of the absolute and relative velocities has been analysed by Margolis⁴. The objective of this damper-control scheme is to attain maximum damping force from the damper when it acts to reduce the amplitude of mass acceleration and damping force is reduced to a minimum when it acts to increase the magnitude of mass acceleration.

The sequential damping mechanism can be realised by implementing a two-position on-off valve to a conventional hydraulic damper. The on-off valve utilises feedback signals of relative velocity and either absolute velocity or relative displacement response of the isolator.

2.1 Sequential Damper Model

Alternatively, a variation in damping is realised by appropriately tuned, externally mounted pressure relief valves where command signal is generated from pressure differentials, P_{12} . From the Eqns (2) and (3), it can be seen that the ratio of P_{12} and P_{32} is a constant.

$$\lambda = P_{32} / P_{12} \quad (6)$$

From the Eqns (1), (5), and (6), the damping force, F_d is obtained as a function of P_{12} :

$$F_d = \alpha P_{12} \quad (7)$$

where

$$\alpha = A_p + \lambda A_r$$

From the Eqns (2) and (7), it is evident that P_{12} , and thus the damping force, are dependent upon the square of relative velocity across the piston. Magnitude of vibration becomes predominant at high excitation frequencies, and thus yields poor vibration isolation. The Eqn (7) shows that magnitude of damping force at higher excitation frequencies can be reduced by limiting pressure differential across the piston in a manner similar to on-off dampers.

Thus, a passive sequential damper is modelled such that damping force is reduced when P_{12} exceeds a preset value of pressure differential across the piston $(P_{12})_o$. Sequential damping is modelled by introducing compression/rebound pressure relief valves to the hydraulic damper. Compression and expansion relief valves are introduced across rebound and compression chambers such that the relief valve remains closed when $|P_{12}| < (P_{12})_o$, and thus, the damper acts as a constant-orifice damper to provide high damping. The relief valve opens when the magnitude of instantaneous pressure

differential, P_{12} exceeds the preset value $(P_{12})_0$. An ideal sequential damping scheme is thus configured while neglecting the dynamics due to pressure relief valves:

$$\left. \begin{aligned} F_d &= \alpha P_{12} \quad \text{for } |P_{12}| < (P_{12})_0 \\ F_d &= \alpha P_{12} \text{ sign}(P_{12}) \quad \text{for } |P_{12}| > (P_{12})_0 \end{aligned} \right\} \quad (8)$$

In view of vehicle vibration isolation, it is desirable to determine the appropriate value of limiting pressure $(P_{12})_0$, such that a high damping is generated around resonant frequency, and the damping force is reduced considerably at higher frequencies. For convenience of analysis, a damping parameter is defined as the ratio of damping force to linear critical damping force of a 1-DOF system⁵.

$$\xi = \frac{F_d}{2\dot{Z}\sqrt{mK_s}} \quad (9)$$

Damping parameter for a constant-orifice damper can be expressed from the Eqns (2), (5), (7), and (9) as

$$\xi = \frac{\alpha}{2\sqrt{mK_s}} \left[\frac{\rho}{2n^2 C^2_{d1}} \right] \left[\frac{A_p}{A_{n1}} \right] |\dot{Z}| \quad (10)$$

From Eqn (10) reveals that the damping parameter for to a constant-orifice damper is no longer constant but proportional to the magnitude of relative velocity across the damper.

Damping parameter for a passive sequential damper is expressed from the Eqns (2), (5), (8), and (10) as

$$\left. \begin{aligned} \xi &= \frac{\alpha}{2\sqrt{mK_s}} \left[\frac{\rho}{2n^2 C^2_{d1}} \right] \left[\frac{A_p}{A_{n1}} \right] |\dot{Z}| \\ &: \text{for } |P_{12}| < (P_{12})_0 \\ \xi &= \frac{\alpha(P_{12})_0}{2\sqrt{mK_s} |\dot{Z}|} \quad \text{otherwise} \end{aligned} \right\} \quad (11)$$

The Eqn (11) reveals that the damping parameter of a sequential damper is proportional to the magnitude of relative velocity for $|P_{12}| > (P_{12})_0$, as in the case of constant-orifice damper. However as the relative velocity increases, magnitude of pressure differential, P_{12} exceeds the limiting value $(P_{12})_0$ and corresponding damping parameter is then obtained as inversely proportional to the magnitude of the relative velocity.

Externally mounted pressure relief valves need to be tuned to achieve variable damping characteristics to suit varying applications, and terrain profiles, an initial estimate of limiting pressure $(P_{12})_0$ can be obtained from the response of linear system. For a base-excited 1-DOF linear system, maximum value of damping ratio ξ_{\max} is determined in view of desirable response, corresponding to undamped natural frequency. The damping ratio can be related to relative velocity transmissibility at $\omega = \omega_n$ in the following manner^{5, 6}:

$$\xi_{\max} = \frac{|\dot{\chi}_s|}{2|\dot{Z}|} \quad \text{at } \omega = \omega_n \quad (12)$$

For effective vehicle suspension, it is desirable to achieve appropriate control of resonant peak. The minimum value of limiting pressure corresponding to natural frequency is thus obtained from the Eqns (11) and (12) as

$$(P_{12})_0 = \frac{K_s \chi_s}{\alpha} \quad \text{at } \omega = \omega_n \quad (13)$$

However, to get effective vibration isolation performance, the limiting pressure may be selected as

$$(P_{12})_0 = tf (P_{12})_0 \quad \text{at } \omega = \omega_n \quad (14)$$

here, tf is the pressure limiting tuning factor for sequential damper.

The equations for hydraulic damper are solved for 1-DOF system subject to harmonic displacement excitation at its base via numerical integration.

3. ANALYTICAL MODELLING & SHOCK AND VIBRATION ISOLATION PERFORMANCE OF VEHICLE SUSPENSION SYSTEM

3.1 Dynamic Response of 4-DOFs Half-car Vehicle System

In this study, vehicle suspension equipped with passive sequential damper and constant-orifice hydraulic damper is modeled as a half-car model (4-DOFs) system. This model has been analysed to evaluate vehicle shock and vibration isolation performance to demonstrate ride performance potentials of the sequential damper.

To simplify the mathematical treatment of these vehicle models, the following assumptions have been made:

- (a) Vehicle forward speed is constant
- (b) Tyres do not leave the ground
- (c) Tyres are modelled as linear springs
- (d) Hysteretic properties of the tyres are assumed to be small
- (e) Suspension deflections are small
- (f) All spring rates of the system are assumed to be constant excepting the gas spring rate.

3.2 Equations of Motion for a 4-DOFs Half-car Vehicle System

The schematic diagram for the vehicle body modelled as 4-DOFs is shown in the Fig. 3. The equations of motion for 4-DOFs half-car vehicle model for passive nonlinear system are given as

(a) Sprung mass

$$m_s \ddot{\chi}_s + K_{sf}(\chi_{sf} - \chi_{uf}) + F_{Df}(t) + K_{sr}(\chi_{sr} - \chi_{ur}) + F_{Dr}(t) = 0 \quad (15)$$

(b) Unsprung mass-front wheel

$$m_{uf} \ddot{\chi}_{uf} - K_{sf}(\chi_{sf} - \chi_{uf}) - F_{Df}(t) + K_{if}(\chi_{sf} - \chi_{uf}) = 0 \quad (16)$$

(c) Unsprung mass-rear wheel

$$m_{ur} \ddot{\chi}_{ur} - K_{sr}(\chi_{sr} - \chi_{ur}) - F_{Dr}(t) + K_{ir}(\chi_{sr} - \chi_{ur}) = 0 \quad (17)$$

(d) Equation for pitching motion

$$I_p \ddot{\theta}_p + K_{sf}(\chi_{sf} - \chi_{uf})l_f + F_{Df}(t)l_f - K_{sr}(\chi_{sr} - \chi_{ur})l_r + F_{Dr}(t)l_r = 0 \quad (18)$$

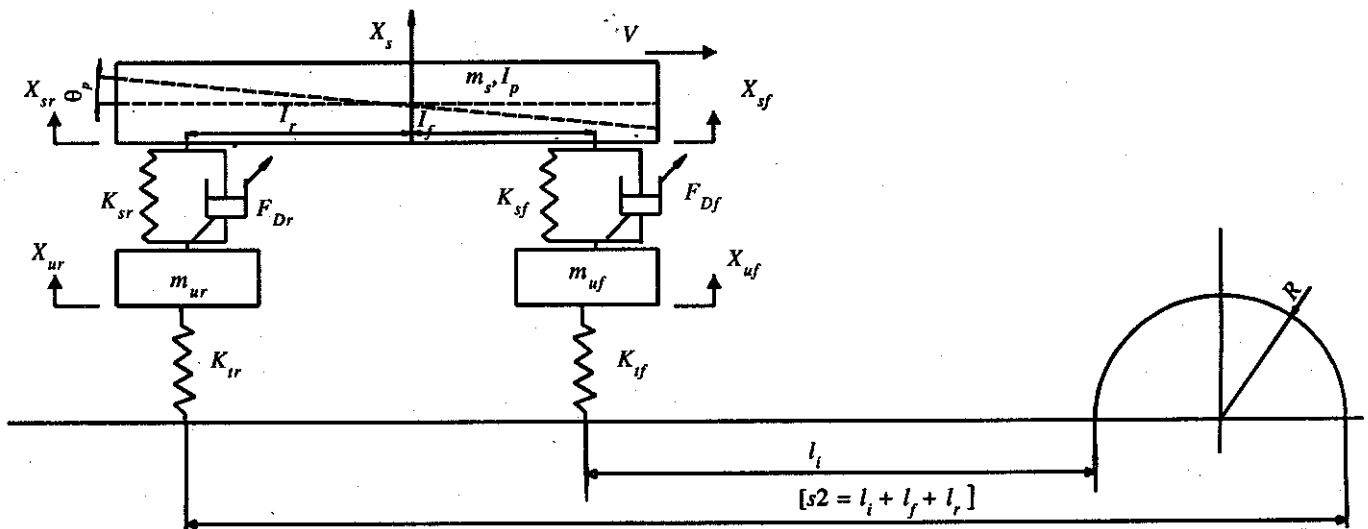


Figure 3. Half-car model with half-round obstacle

It is assumed that the pitch angle is small, so one can write

$$\chi_{sf} = \chi_{sf} + l_f \theta_p$$

$$\chi_{sr} = \chi_{sf} - l_r \theta_p$$

The set of Eqns (15), (16), (17), and (18) describes the dynamic behaviour of sequential and constant orifice dampers.

4. COMPUTER SIMULATION

Dynamic ride performance of vehicle suspension employing passive sequential damper has been evaluated through shock isolation characteristics for half-car vehicle model (Fig. 4). It has been observed from displacement transmissibility curve of 1-DOF model in Fig. 5, that the best isolation is achieved when the tf is 1.0. Hence $tf = 1.0$ is taken in the analysis of sequential damper for the half-car model. The vibration isolation performance of the sequential damper is evaluated in terms of displacement and velocity transmissibility ratio and compared to those of constant-orifice damper. The nonlinear differential equations of motion of 4-DOFs half-car model subjected to harmonic displacement at its base, is solved via numerical integration. Vibration transmissibility characteristics of the nonlinear system are determined as ratio of steady state response amplitude to constant excitation amplitude at each excitation frequency. The shock isolation performance for 4-DOFs vehicle model is predicted for half-round obstacle of radius 0.1524 m, sinusoidal input amplitude of 0.1524 m, and steep ramp input of 0.1524 m. Numerical simulation has been carried out for constant-orifice damper using two orifices, and sequential damper using two orifices and pressure limiting tuning factor $tf=1.0$. Shock and vibration isolation performance of constant-orifice damper and sequential damper for half-car vehicle system has been investigated for forward speed of vehicle 11.11 m/s and with the parameters given in Tables 1 and 2.

4.1 Vibration Isolation Performance

Vibration isolation characteristics of 4-DOFs vehicle model, employing sequential damper are

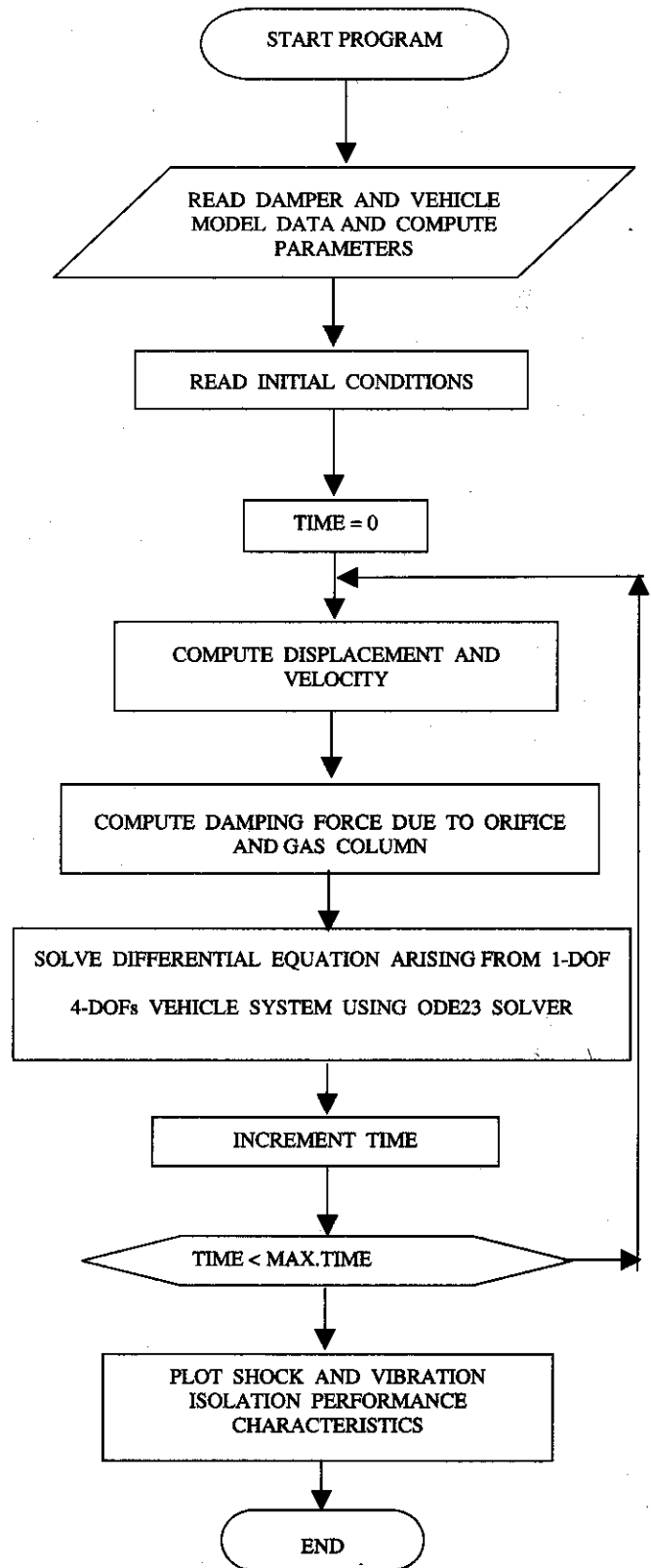


Figure 4. Numerical simulation flow chart for a sequential damper.

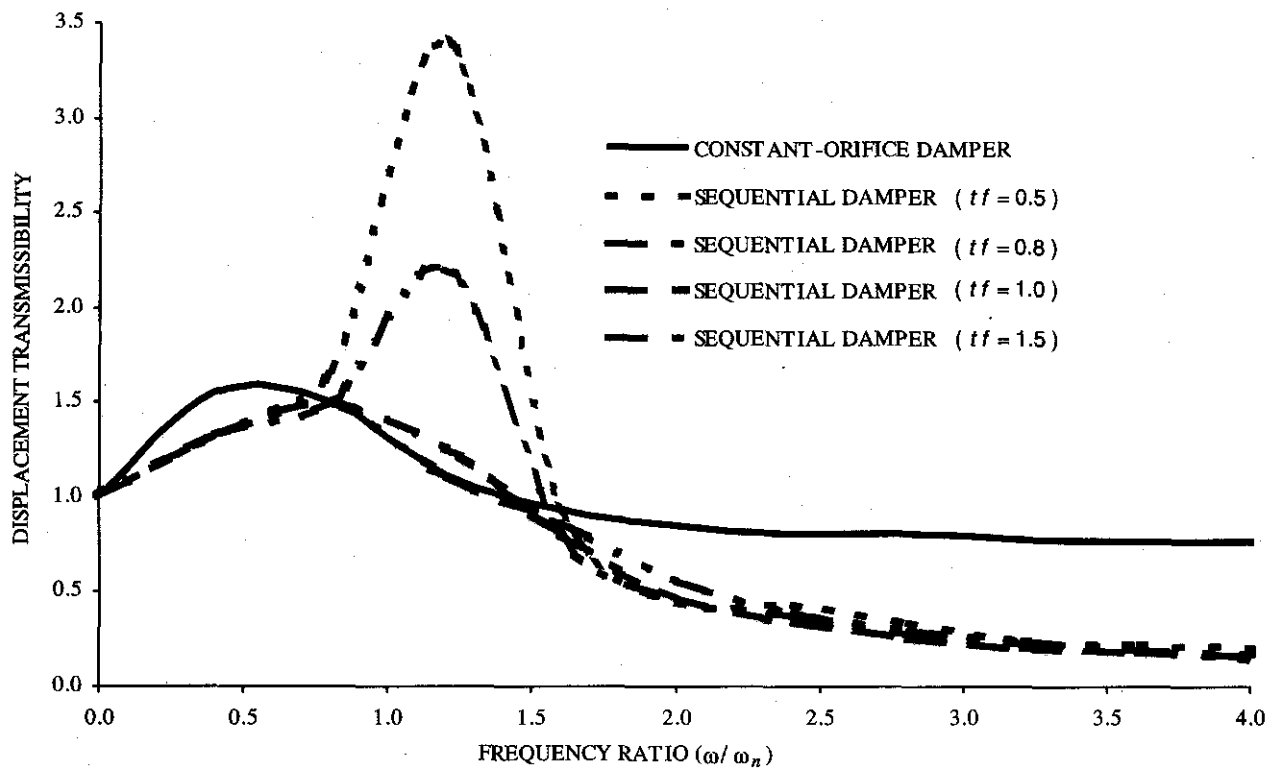


Figure 5. Displacement transmissibility response of 1-DOF system

Table 1. Simulation parameters of sequential and constant-orifice damper for 1-DOF system

Simulation parameter	Value
m_s (kg)	65
K_s (N/m)	4000
ρ (kg/m ³)	797
C_{d1}	0.7
C_{d2}	0.7
A_p (m ²)	2.0268 e -3
A_r (m ²)	1.2667 e -4
A_{n1} (m ²)	1.35 e -5
A_{n2} (m ²)	1.35 e -5
X_r (m)	0.05
n	2
ξ	0.7
P_o (N/m ²)	13.7 e 5
V_o (m ³)	1.9 e -4
v	1.4

Table 2. Simulation parameters for 4-DOFs half-car vehicle system

Simulation parameter	Value
I_p (kg m ²)	1230
m_s (kg)	240
m_{uf} (kg)	36
m_{ur} (kg)	35.5
K_{sf} (N/m)	19960
K_{sr} (N/m)	17550
K_{yf} (N/m)	175500
K_{yr} (N/m)	175500
l_l (m)	0.2524
l_r (m)	1.011
l_r (m)	1.803

Other parameters as mentioned in Table 1 are applicable to Table 2 also.

evaluated for $tf = 1.0$ and $n = 2$. Figure 6 shows displacement transmissibility response of sprung mass (C.G.). Sprung mass (C.G.) displacement transmissibility response of constant orifice

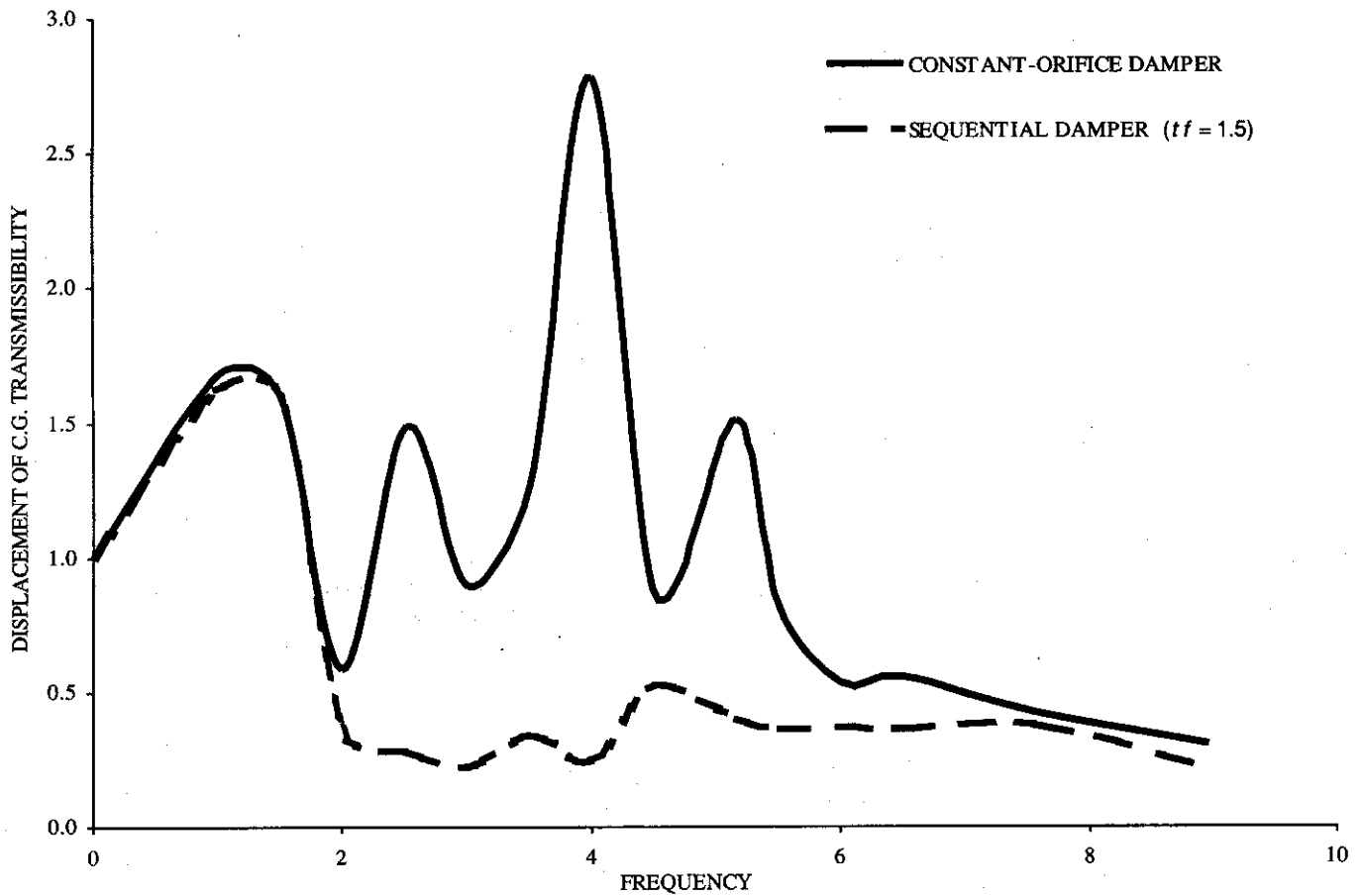


Figure 6. Displacement of C.G. transmissibility response of a 4-DOFs half-car system

exhibits four peaks corresponding to sprung mass displacement. The Transmissibility response of 4-DOFs vehicle model employing sequential damper is identical to constant-orifice damper at low excitation frequencies. The sequential damper continues to dissipate energy identical to constant-orifice damper around first resonant frequency. However, as excitation frequency, and thus the relative velocity response increases, pressure differential P_{12} is held around $(P_{12})_0$ by pressure-relief mechanism to the damping force. Thus, displacement response of sequential response of sequential damper is considerably reduced for higher frequencies.

4.2 Shock Isolation Performance

4.2.1 Half-round Obstacle

The Figs 7 and 8 show the transient response of sprung mass heave and pitch displacement. Both

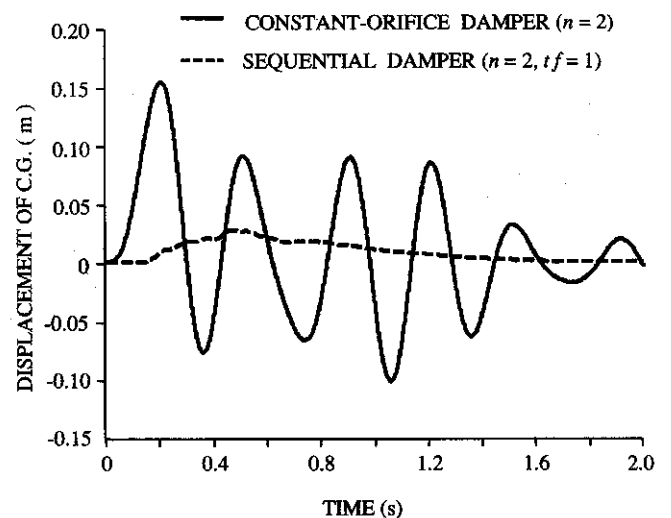


Figure 7. Numerical simulation of 4-DOFs system for half-round obstacle: Transient pitch displacement of C.G. response.

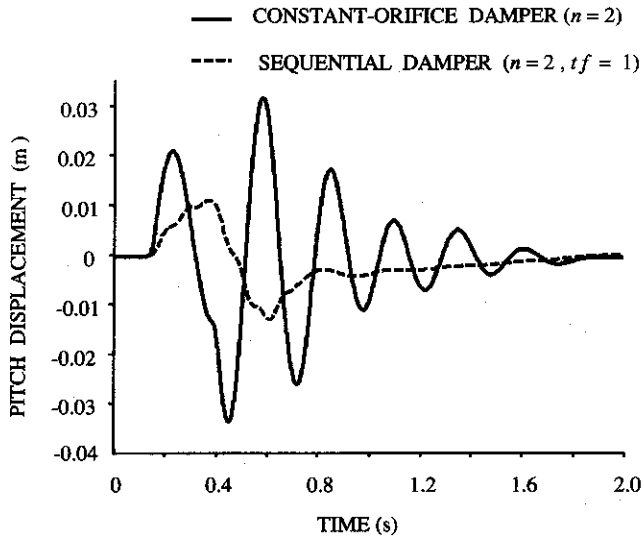


Figure 8. Numerical simulation of 4-DOFs system for half-round obstacle: Transient pitch displacement response.

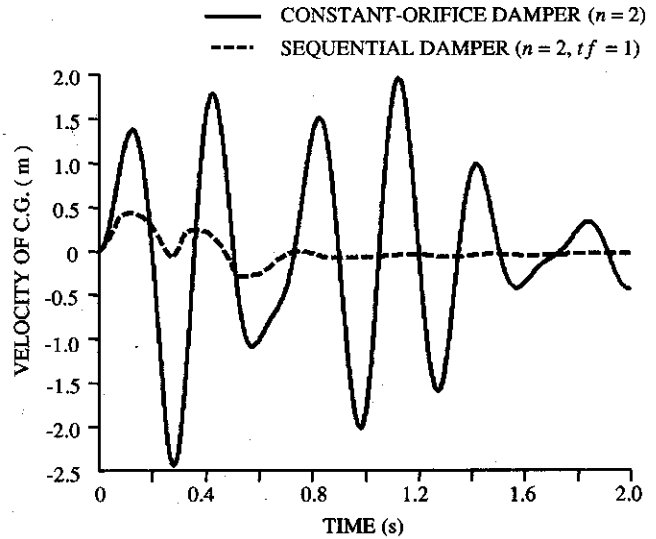


Figure 10. Numerical simulation of 4-DOFs system for sinusoidal obstacle: Transient velocity of C.G. response.

response show that the sprung mass heave and pitch displacement of sequential damper have been greatly improved compared to constant-orifice damper. The settling time for the transient response of the vehicle with sequential damper is very less as compared to that obtained using a constant-orifice damper.

4.2.2 Sinusoidal Bump

Figures 9 to 12 show the transient response of sprung mass heave and pitch displacement, and

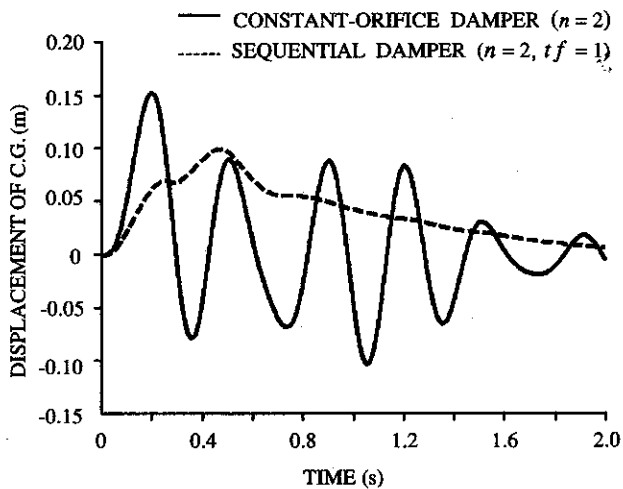


Figure 9. Numerical simulation of 4-DOFs system for half-round obstacle: Transient pitch displacement of C.G. response.

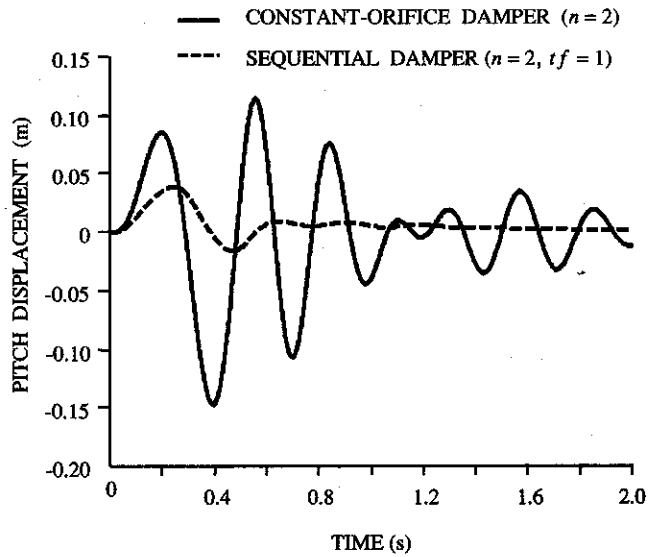


Figure 11. Numerical simulation of 4-DOFs system for sinusoidal obstacle: Transient pitch displacement response.

velocity which shows the results similar to half-round obstacle, and the settling time for the transient response of the vehicle with sequential damper is very less as compared to that obtained using a constant-orifice damper. From the results of the Figs 13 and 14, it is seen that the displacement and velocity of unsprung mass at the front wheel, shows one peak in sequential damper as compared to constant-orifice damper but the sequential damper response of unsprung mass at the front wheel,

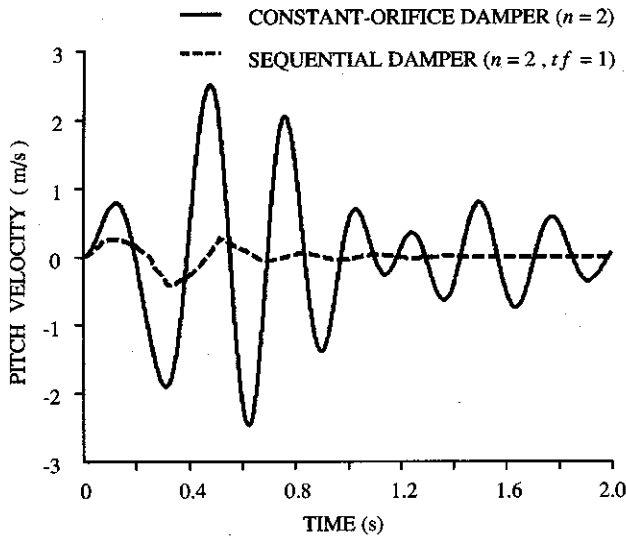


Figure 12. Numerical simulation of 4-DOFs system for sinusoidal obstacle: Transient pitch velocity response.

which has less settling time, is very less as compared to that obtained using a constant-orifice damper. The rear wheel response for the 4-DOFs half-car vehicle model is the same and for other input is similar.

4.2.3 Steep Ramp Input

Step ramp input corresponds to weight transfer onto a wheel during braking and cornering or the

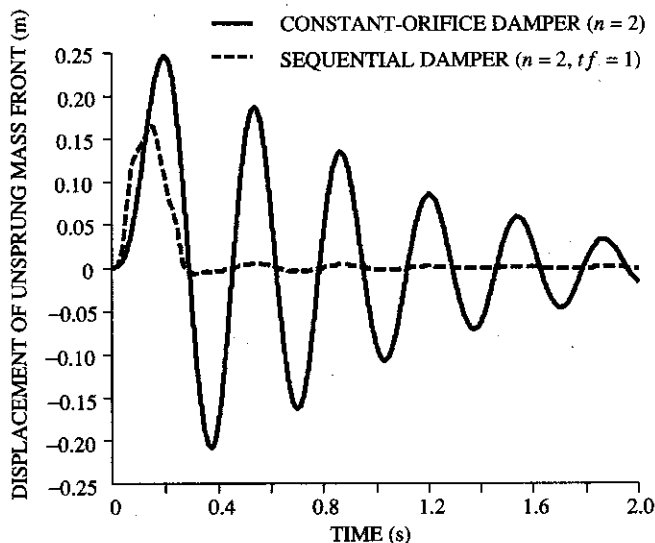


Figure 13. Numerical simulation of 4-DOFs system for sinusoidal obstacle: Transient displacement response of unsprung mass front wheel.

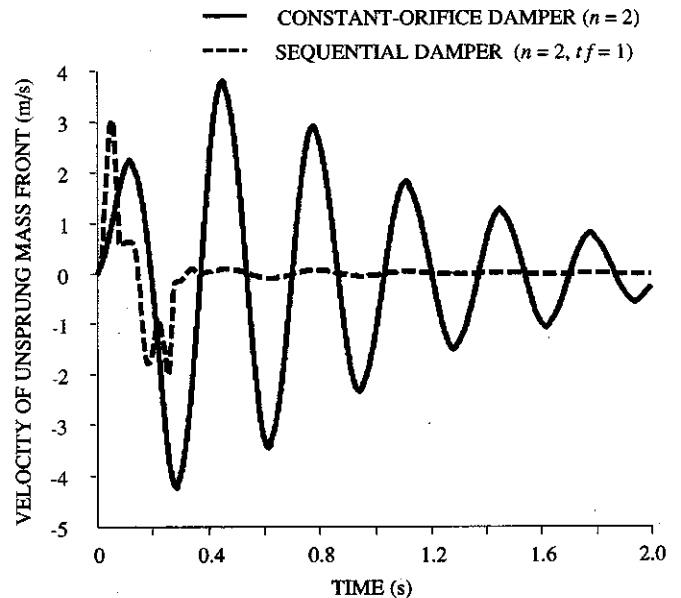


Figure 14. Numerical simulation of 4-DOFs system for steep ramp input: Transient velocity response of C.G. response.

increase in aerodynamic force as the car accelerates. Figures 15 and 16 show transient response of sprung mass heave and pitch displacement. This response shows that the settling time for the transient response of the vehicle with sequential damper is very less as compared to that obtained using a constant-orifice damper.

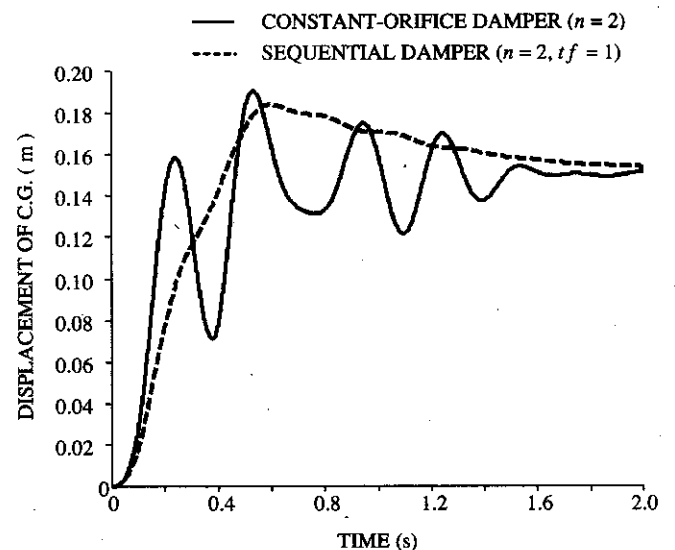


Figure 15. Numerical simulation of 4-DOFs system for steep ramp input: Transient displacement of C.G. response.

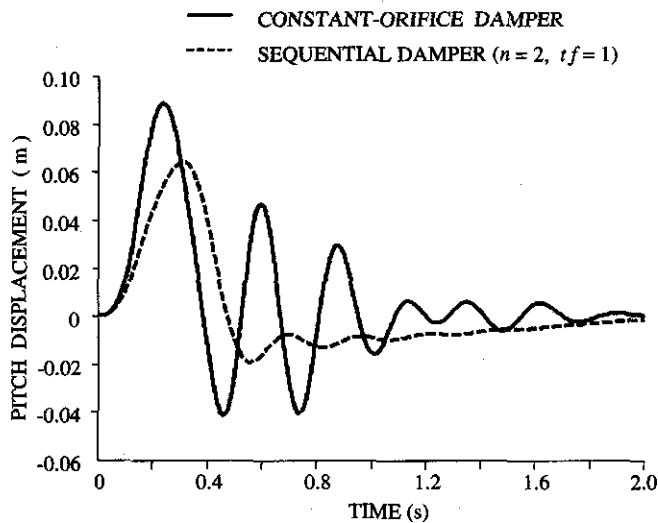


Figure 16. Numerical simulation of 4-DOFs system for steep ramp input: Transient pitch displacement response.

6. CONCLUSION

A tunable sequential damper has been mathematically modelled incorporating the nonlinear restoring and damping forces due to gas column and sequential damping, respectively while the dynamics due to control valve has been neglected. Vibration transmissibility characteristics of a sequential damper have been evaluated and compared to those of a constant-orifice damper. Ride quality improvement potential of a passive sequential damper is investigated via computer simulation for half-round obstacle, sinusoidal, and steep ramp input of a 4-DOFs half-car vehicle model. It can be concluded that passive

sequential damper provides better shock and vibration isolation performance than constant-orifice damper. The shock and vibration isolation performance of a 4-DOFs half-car vehicle model revealed that an adequately tuned sequential damper offers considerable potential to improve the vehicle ride.

REFERENCES

1. Karnopp, D.; Crosby, M.J. & Harwood, R.A. Vibration control using semi-active force generator. *J. Engg. Indus.*, 1974, 619-25.
2. Rakheja, S. & Sankar, T. S. Vibration and shock isolation performance of a semi-active on-off damper, *Transactions of ASME*, 1995, **107**, 398-03.
3. Merritt, H.E. Hydraulic control systems. Wiley, New York, 1967.
4. Margolis, D.L. & Goshtasbpour, M. A chatter of semi-active on-off Suspension and its cure. *In Vehicle system dynamics*, Vol. **13**, 1984, pp. 129-44.
5. Thompson. Theory of vibration with applications. Ed. 2. Prentic Hall, Englewood, Chiffs, 1971.
6. Rekheja, S.; Hong, Su & Sankar, T.S. Analysis of a passive sequential damper for vehicle suspension. *In Vehicle system dynamics*, Vol. **19**, 1990, pp. 289-12.